Arabian Journal of Geosciences (2023) 16:540
https://doi.org/10.1007/s12517-023-11648-y

ORIGINAL PAPER

Temporal characteristics of northeast monsoon rainfall and its teleconnection with the large-scale circulation indices

Harithasree Sreedevan[1] · Subrat Kumar Panda[1] · Kanhu Charan Pattnayak[2,3]

Received: 7 December 2022 / Accepted: 19 August 2023 / Published online: 4 September 2023

Abstract

This study investigates the temporal variability of the northeast monsoon rainfall (NEMR) in India and its relationship with El Niño-Southern Oscillation (ENSO) and the Indian Ocean Dipole (IOD) using wavelet analysis. The results show that NEMR is highly variable, with a coefficient of variation of about 25%, which is due to its dependence on dynamic systems with a wide range of spatial and temporal scales. The temporal variability of NEMR is at different time scales ranging from intra-annual to interannual to decadal time scales. The large-scale circulation features, ENSO and IOD, also exhibit variability at different time scales. El Niño events have a typical frequency range of 2 to 7 years, with a prolonged impact that can last for several months, spreading across the globe. Wavelet transforms of SOI and Nino 3.4 have revealed variability at the time scale of 2–8 years, which is in line with the observed ENSO cycle. The wavelet transform of DMI displays significant variability in short time scales, typically less than 2–4 years. The study also finds a strong negative relationship between NEMR and SOI, recorded in September, especially over Tamil Nadu, Kerala, and Coastal Andhra Pradesh during the periods 1900–1920 and 1980–2000. This correlation is strong at time scales of 2–4 years and 4–8 years during the periods 1880–1920, possibly related to the ENSO cycle and the oscillation of anomalous SST over the Indian Ocean. The study highlights the need for further studies to understand the physical processes that contribute to the observed variability in El Niño and other ocean–atmosphere interactions.

Keywords Northeast monsoon · El-Nino Southern Oscillation · Southern Oscillation Index · Dipole mode index · Wavelet power spectrum · Wavelet coherence

Introduction

The Indian Monsoon is comprised of two vital monsoons: the Southwest Monsoon, which occurs from June to September, and the northeast monsoon (NEM), which occurs from October to December (OND). The monsoon precipitation is crucial because it control many sectors, including agriculture, food, energy, and water, as well as disaster management. The spatial and temporal variability of monsoon rainfall is highly uncertain at multiple scales. The India Meteorological Department (IMD) identifies the period from October to December as the Northeast monsoon. NEM is a component of the Northeast trade winds that develop due to the temperature gradient (Dhar and Rakhecha 1983). In comparison to the summer monsoon, the NEM is drier, more stable, and has a smaller vertical extent. During NEM, rainfall occurs in the meteorological subdivisions of Tamil Nadu (TN), Kerala (KER), Coastal Andhra Pradesh (CAP), Rayalaseema (RYS), and South Interior Karnataka (SIK).

Tamil Nadu receives 48% of its annual rainfall during the NEM season, making it the primary rainy season. The average date of occurrence of NEM over the coasts of Tamil Nadu and Andhra Pradesh is October 20. (Balachandran et al. 2020). During this time, cyclones may form over the Bay of Bengal and the Arabian Sea, which has a significant impact on precipitation. Thus,

Responsible Editor: Zhihua Zhang

✉ Subrat Kumar Panda
subrat.atmos@curaj.ac.in

[1] Department of Atmospheric Science, School of Earth Sciences, Central University of Rajasthan, Kishangarh, Rajasthan, India

[2] School of Earth and Environment, University of Leeds, Leeds, UK

[3] Centre for Climate Research Singapore, Meteorological Service Singapore, Singapore, Singapore

northeast monsoon rainfall (NEMR) exhibits a high degree of variability with a coefficient of variation of 25%, with approximately 11% of NEMR variation attributable to precipitation associated with the passage of cyclones and depressions (Geetha and Raj 2015). NEMR is also affected by global climate parameters such as El Nino, La Nina, Southern Oscillation (Bjerknes 1969), Indian Ocean Dipole (IOD) (Saji et al. 1999), and Madden–Julian Oscillation (MJO) (Madden and Julian 1971). El Nino, a positive IOD, and MJO phases 2–4 with amplitudes greater than 1 are usually associated with favorable NEMR (Madden and Julian, 1972).

Numerous research studies have shown that the El Niño-Southern Oscillation (ENSO) significantly affects the interannual variability of NEMR. In recent years, (Zubair and Ropelewski 2006) and Kumar et al. (2007) demonstrated a correlation between ENSO and NEM precipitation over South Asia. Kumar et al. (2007) identified stronger anomalies in the easterlies and anomalous convergence of moisture in the lower levels over the North Indian Ocean and stated that these could be the cause of the observed strengthening. According to a study by (Kripalani and Kumar 2004), there is a positive correlation between NEMR and IOD in the South Peninsular region, resulting in increased precipitation during the positive IOD phase and vice versa. Kumar and Hoerling (2003) discovered a correlation between the mean monthly sea surface temperature (SST) over the Nino-3.4 region in August and September over a 50-year period and the winter monsoon rainfall over Central Asia Plateau. This is due to the fact that ENSO influences the tropospheric circulation (Bjerknes, 1966). In spite of the fact that the NE monsoon rainfall is significantly influenced by the favorable large-scale circulation caused by the Pacific, the local air-sea interaction is crucial in influencing or causing the extreme rainfall events connected to El Nino (Singh et al. 2017). George et al. (2011) discovered a correlation between the dipole mode index (DMI) and the NEMR. Ashok et al. (2001) and Rao (1976) demonstrated that the SST variability between the west and east sides of the Equatorial Indian Ocean undergoes rapid fluctuations that result in interannual variability, whereas the predominant SST variability has an average 3–5-year cycle. Yasunari and Seki (1992) demonstrate that the lag cross-correlations between the Southern Oscillation Index (SOI) and the NEMR in India fluctuate similarly to those between SST in the tropical Pacific and the Indian summer monsoon rainfall. The northeast monsoon over India is influenced by several large-scale climate patterns, including the El Niño Southern Oscillation (ENSO) and the Indian Ocean Dipole (IOD) (Rajeevan et al 2012).

Very limited studies (Rajeevan et al. 2012; Kripalani and Kumar 2004; George et al. 2011) are available on the variability of NEMR owing to its high variability as opposed to the Indian summer monsoon whose spatial and temporal characteristics (Das et al. 2011; Deka et al. 2013; Jain et al. 2013; Das et al. 2015; Goswami et al. 2003; Goswami et al. 2006, Hu and Nitta 1996) have been well explored and established. The objective of this study is to understand the temporal characteristics of NEMR and its teleconnection with the large-scale circulation indices using wavelet analysis for the period 1871–2016. Wavelet analysis is a mathematical tool used to study the temporal characteristics of time series data. It allows researchers to analyze the frequency and time-dependent behavior of a dataset and identify any cyclical patterns or trends that may exist (Torrence and Compo 1998). This study illustrates the application of wavelets to study the variability of the systems under study. Studies (Kumar and Hoerling 2003, 2007; Zubair and Ropelewski 2006; Yasunari and Seki 1992, Tomita and Yasunari 1996, Rathinasamy et al. 2019) identifying the relationship between NEMR and circulation features like ENSO and IOD focus mainly on the nature of the relationship whereas this study also focuses on how this relationship has fluctuated with time over the years during the period of study. Overall, research on the temporal and spatial characteristics of NEM rainfall and its teleconnection with large-scale circulation indices using wavelet analysis has provided insights into the mechanisms that drive this important seasonal rainfall pattern and may help improve forecasting capabilities in the future. The manuscript has been divided into distinct sections. The data and study area are described in the "Data and study area" section, while the methodology used to achieve this research objective is described in the "Methodology" section. The "Result and discussion" section describes the results and discussion, and the "Conclusions" section is the conclusion.

Data and study area

The study area includes the five meteorological subdivisions that receive the NEMR namely Tamil Nadu, Rayalaseema, Coastal Andhra Pradesh, South Interior Karnataka, and Kerala. The long-term rainfall sub-divisional Homogeneous Indian Monthly Rainfall Datasets (Parthasarathy et al. 1993) for the period of 1871–2016 used in the study. These measurements of rainfall were made by the network of rain gauge stations set up by the India Meteorological Department. The circulation indices that have been used in this study are the Southern Oscillation Index, Nino 3.4 Index, and Dipole Mode Index (DMI).

The Southern Oscillation Index (SOI, Walker 1924) is a standardized index describing the state of the Southern Oscillation by the pressure differences between Tahiti and Darwin, Australia. When SOI is negative (positive), the

atmospheric pressure over Tahiti is below (above) normal and over Darwin, it is above (below) normal. When the SOI values prolong below − 8, it indicates El Nino event and when values above + 8 sustain, a La-Nina event is said to have occurred. Studies have shown that the periods of events match well with the anomalous changes in temperature in the eastern Tropical Pacific Ocean. Abnormally warm (cold) SST in the eastern tropical Pacific Ocean are observed during negative (positive) SOI values indicating El Niño (La Niña) phenomenon. The SOI data for the period 1871–2016, used in this study was recorded by the Climate Research Unit (CRU, Harris et al. 2014) of University of East Anglia. The time series of the SOI are reflected well as changes in ocean temperatures across the eastern tropical Pacific.

The Niño 3.4 index was obtained from NOAA ESRL Physical Sciences Laboratory (Hansen et al. 1998) for the period 1950–2016. It is also an index used to measure the ENSO effect. It is the 5-month running average anomaly in the sea surface temperature enclosed within the 5° N to 5° S, from 170° W to 120° W extent. When this measure crosses ± 0.4 °C, El Niño/La Niña is said to have occurred (Schneider et al. 2013).

The DMI, put forth by Saji et al. (1999), is an indicator of the SST gradient across the east and west tropical Indian Ocean, associated with the Indian Ocean Dipole. The Indian Ocean DMI is defined as the anomalous SST gradient between the western equatorial Indian Ocean over the 50° E–70° E and 10° S–10° N box and the south eastern equatorial Indian Ocean over 90° E–110° E and 10° S–0° N box. The DMI data for this study was obtained from NOAA ESRL Physical Sciences Laboratory (Hansen et al. 1998) for the period 1871–2016. The Fig. 1 shows the five meteorological subdivisions that receive the NEMR namely Tamil Nadu, Rayalaseema, Coastal Andhra Pradesh, South Interior Karnataka, and Kerala (Fig. 1).

Methodology

The wavelet analysis has been used in this study to analyze the variability of the NEMR over the period 1871–2016 and its variability with respect to El Nino and Indian Ocean Dipole. Wavelet analysis (Schmidbauer and Roesch 2018) is a popular time–frequency analysis technique that is widely used to study the statistical properties of the non-stationary signals, here the signal being the long-term NEMR time series from 1871–2016.

The wavelet transform uses a wavelet function and computes the similarity between the input time series and the wavelet function. This correlation is computed separately for different time intervals, thus resulting in a representation containing information about the frequencies and the point of time at which each of the frequencies occurred. The magnitude of the wavelet spectrum coefficients shows how well the wavelet matches with the time

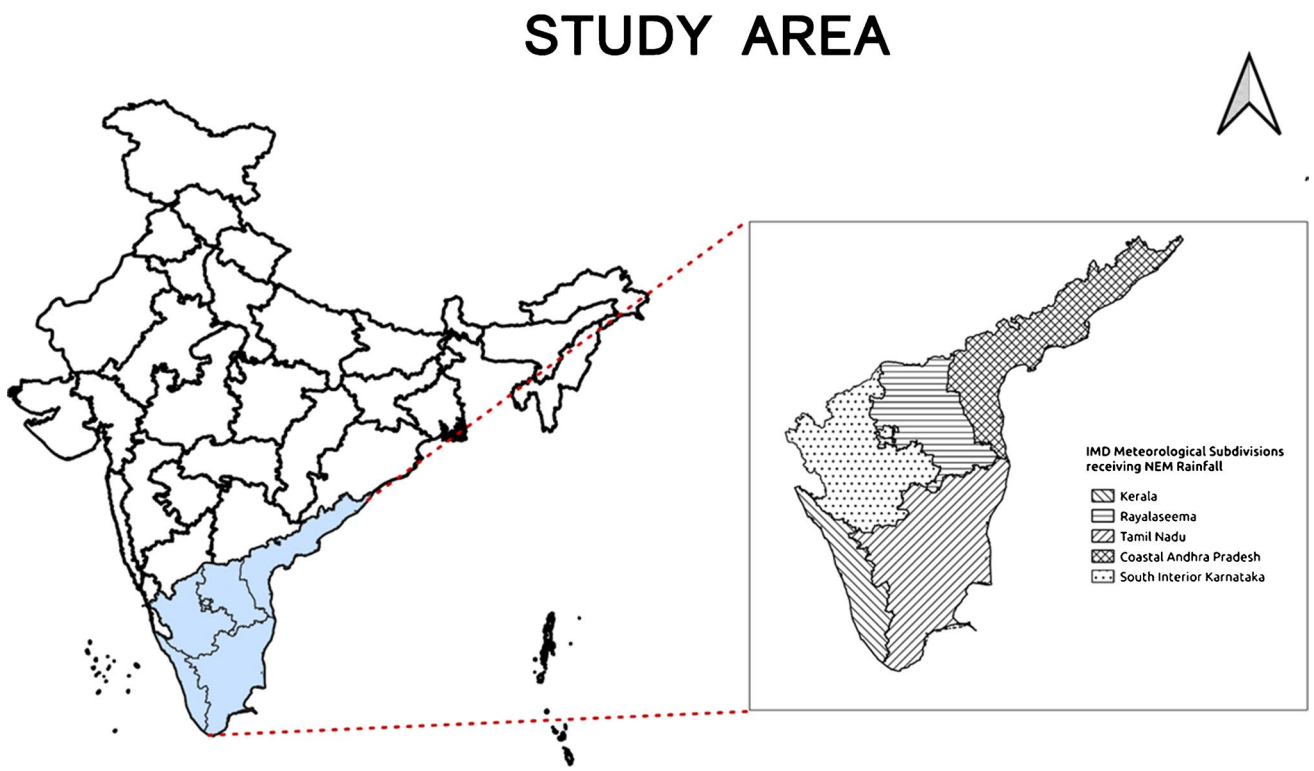

Fig. 1 Study area consisting of the five meteorological subdivisions that receives rainfall during northeast monsoon season

series. At each scale, the wavelet spectrum coefficients also depict the amplitude of a time series.

The power spectrum of a time series also describes the distribution of the wavelet power into frequency components of the time series. It can be used to detect the seasonality present in the data, wherein the spectrum will show peaks at the seasonal frequencies.

Morlet wavelet

The Morlet wavelet transform is a mathematical technique used to analyze the time–frequency content of a time series signal. It is based on the convolution of the signal with a set of wavelets, each of which is generated by shifting and scaling a "mother" wavelet function.

The Morlet wavelet is one such mother wavelet function, defined as:

$$\psi(t) = \pi^{0.25} e^{(i*6*t)} e^{(-t^{2/2})} \quad (1)$$

where π is the mathematical constant *pi*, *i* is the imaginary unit, *t* is the dimensionless time, and 6 is the wavenumber which satisfies the admissibility condition. In practice, the value of 6 is commonly used for the Morlet wavelet.

$$S_j = s_0 2^{ij}, \text{where j} = 1, 2, 3 \quad (2)$$

$$j = j^{-1} log_2 \left(Nt/s_0\right) \quad (3)$$

To perform the Morlet wavelet, transform, the input time series is convolved with the Morlet wavelet function, which has been shifted in time and scaled by a factor τ and *s*, respectively. The scaling factor *s* is chosen to be a power-of-two multiple of the smallest resolvable scale, *s*0, which is some multiple of the time resolution dt of the data. For seasonal data with $dt = 0.25$ years, the smallest resolvable scale is $s0 = 0.5$ years.

The wavelet power spectrum (WPS) is computed from the convolution of the input signal with the wavelet family. The WPS indicates the time-varying frequency content of the input signal. The regions with high wavelet power correspond to significant features of the signal, and can be used to identify trends, periodicities, and anomalies in the data.

Wavelet coherence

Wavelet coherence is used to estimate the association between two phenomena. It can be used to study the coherence and phase lag between two time series as a function of time and frequency (Chang and Glover 2010) In this study, it has been used to find the relationship between the NEMR and the climate indices used in this study.

The wavelet coherence of two time series *x* and *y* is

$$R^2 = \frac{| S(C_x^*(a,b)C_y(a,b)) |^2}{S(| (C_x(a,b) |)^2 \times S(| (C_x(a,b) |)^2}$$

where $C_x(a,b)$ and $C_y(a,b)$ denote the continuous wavelet transforms of *x* and *y* at scales *a* and positions *b* (Torrence and Compo 1998). C^*_x is a complex conjugate used as a smoothing operator in time and scale.

Result and discussion

NEMR is highly variable with coefficient of variation of about 25% due to its dependence on dynamic systems with a wide range of spatial and temporal scales. This temporal variability is at different time scales ranging from intra-annual to interannual to decadal time scales. The discussion consists of two sections, one discussing the temporal characteristics of NEMR and the circulation features taken for study, namely, ENSO and IOD. The other section discusses the teleconnection of NEMR with those circulation features.

Temporal variability of NEMR

The wavelet power spectrum of the OND rainfall over the five rainfall subdivisions show high wavelet power in the lower Fourier periods showing their intra-annual variability. The white contours show areas of significance and the areas marked with dashed black lines show the wavelet ridges. Ridges are locations at which the frequency of the scaled wavelet coincides with the local frequency of the signal, that is they are the local maxima of the amplitude of the wavelet transform.

From Fig. 2, we find that the time scales shorter than 2 years are dominant in the variations over nearly all the time domains. All the rainfall subdivisions show dominant variations within the time scales of 2–4 years during the period 1871–1950. Kerala shows significant decadal variations in the time scale of 16–32 years throughout the period of study. CAP shows variability at timescales of 8–16 years during the period 1871–2000. Strong variability is seen in the 2–4 time scale especially during the period 1900–1950.

The average wavelet power shows the power averages across time of a time series. The vertical axis shows the Fourier periods. The horizontal axis shows the averages. The average wavelet power shows significant variations in 2–4 years' timescale at 90% (blue) and 95% (red) confidence. Tamil Nadu and Kerala show strong variations at 8–16 and 16–32 years' time scales, respectively.

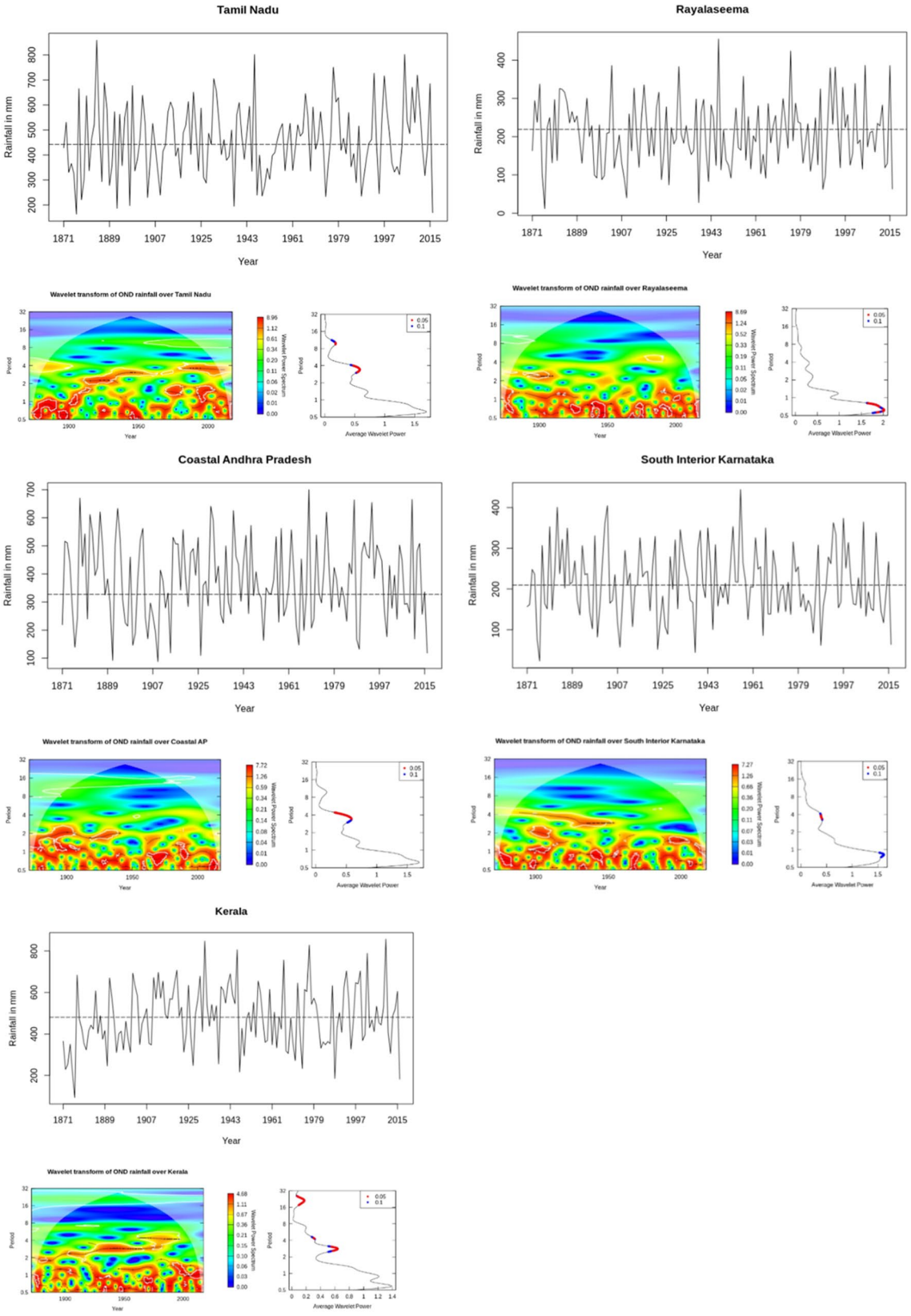

Fig. 2 Wavelet spectrum of OND rainfall over each of the five meteorological subdivisions for the period 1871–2016

Temporal variability of the large-scale circulation features

El Niño events are a complex ocean–atmosphere interaction that occur irregularly, with a typical frequency range of 2 to 7 years. These events start from March, peak between November and January, and have a prolonged impact that can last for several months, spreading across the globe. Previous research by Schneider et al. (2013) has confirmed the variability of El Niño events at time scales of 2–8 years, which is consistent with the observed ENSO cycle. However, it is important to note that the occurrence of El Niño is not exclusively dependent on these time scales and may be influenced by other factors such as oceanic and atmospheric conditions.

Wavelet transforms of SOI (Southern Oscillation Index) and Nino 3.4 have revealed variability at the time scale of 2–8 years, which is in line with the observed ENSO cycle. This is shown in Fig. 3 and supports the findings of Schneider et al. (2013). The wavelet transform of DMI (Indian Ocean Dipole Mode Index) displays significant variability in short time scales, typically less than 2–4 years. These highlights strong fluctuations in the Indian Ocean SST (sea surface temperature) at this time scale, which coincides with the time scale of SST variability of an average of 3–5 year cycles as found in studies by Ashok et al. (2001) and Rao (1976).

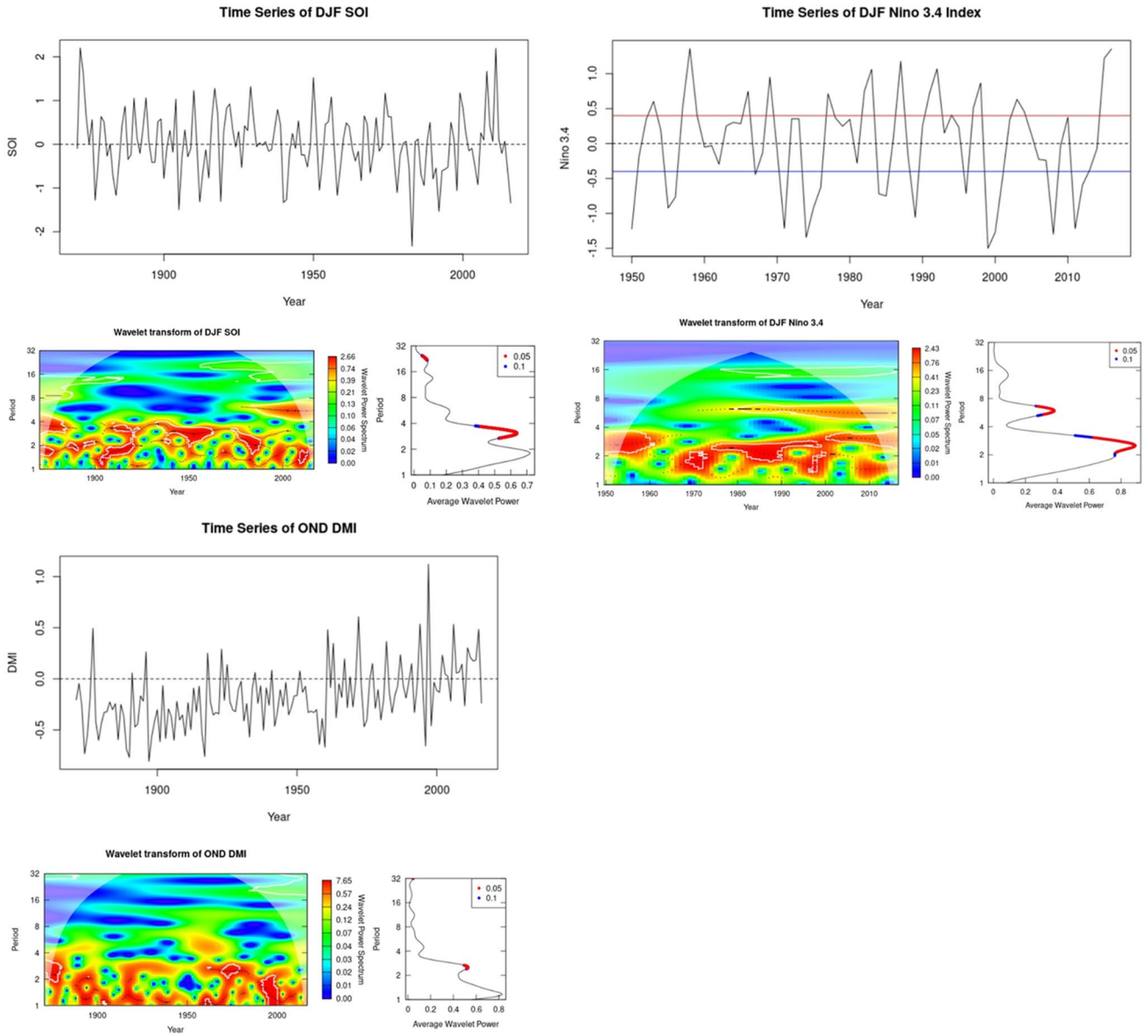

Fig. 3 Wavelet spectrum of DJF SOI, DJF Nino 3.4 Index, and OND DMI for the period 1871–2016

It is worth noting that while wavelet transforms provide insights into the temporal variability of climatic systems, they do not necessarily reveal the underlying mechanisms driving these changes. Therefore, further studies are needed to understand the physical processes that contribute to the observed variability in El Niño and other ocean–atmosphere interactions. Such studies may involve the use of advanced modeling techniques and the integration of multiple datasets to gain a more comprehensive understanding of these complex phenomena.

Teleconnections: NEMR and ENSO

Wavelet coherence is used to determine the time–frequency space where the two NEMR and the circulation indices covary. The warmer colors (red) represent regions with significant association, while colder colors (blue) signify lower correlation between the series. The phase arrows show the relative phasing of two time series, that is they represent the lead/lag phase relations between the series. Arrows point to the right (left) when the time series are in phase (anti-phase). Arrows pointing to the right-down or left-up indicate that the first variable is leading, while arrows pointing to the right-up or left-down show that the second variable is leading (Aguiar-Conraria and Soares 2011).

The figures demonstrate the relationship between ENSO cycle and rainfall variations in India. The black contours in the figures represent 95% significant correlation, while the arrows indicate the relative phase between the series. Through wavelet coherence plots using the Nino 3.4 index and SOI index, Figs. 4 and 5 show the role of ENSO cycle in rainfall variations in India at different time scales. The figures reveal a strong negative relationship between NEMR and SOI, recorded in September, especially over Tamil Nadu, Kerala, and Coastal Andhra Pradesh during

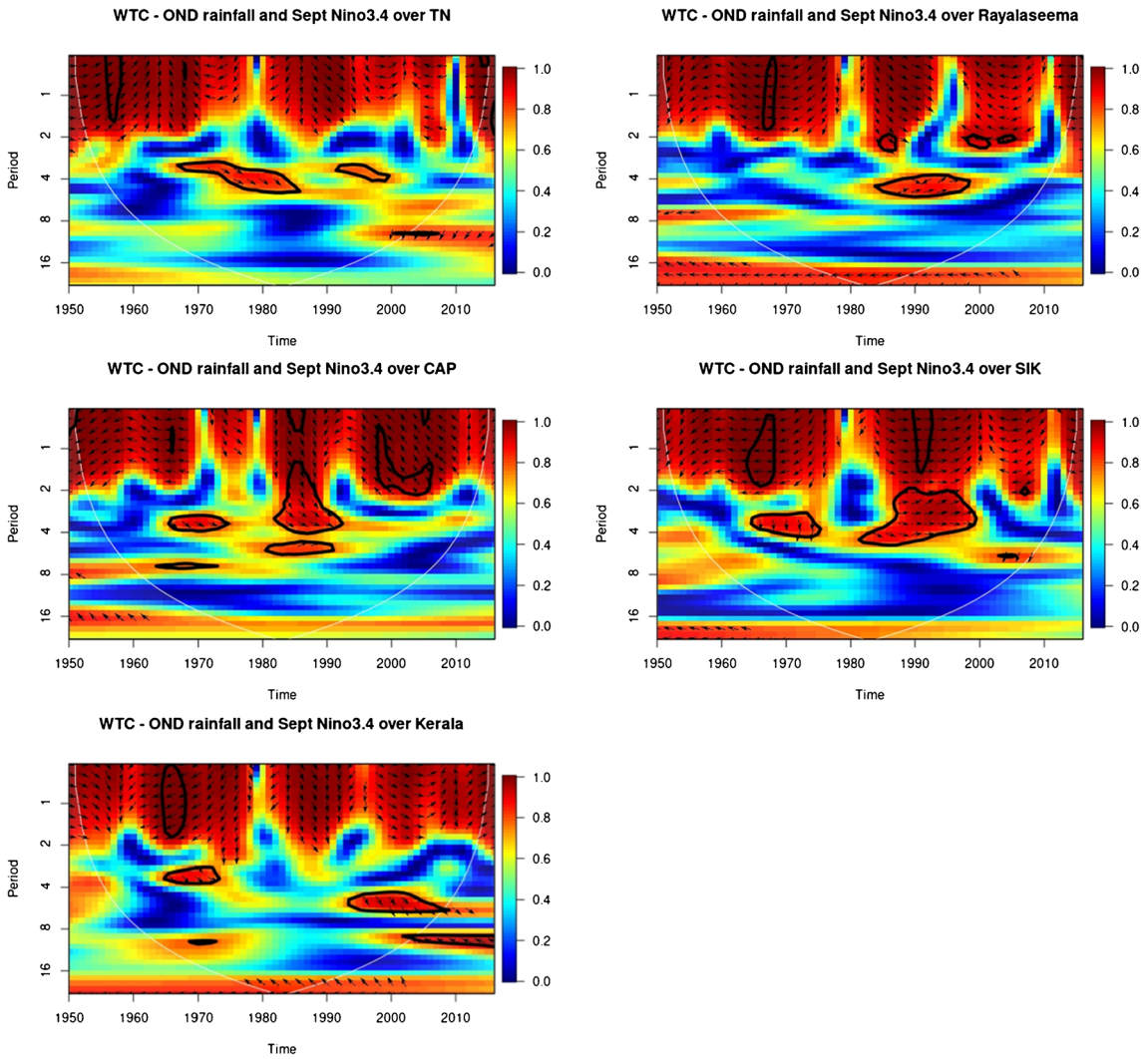

Fig. 4 Wavelet coherence between OND rainfall and September Nino 3.4 Index over each of the five meteorological subdivisions

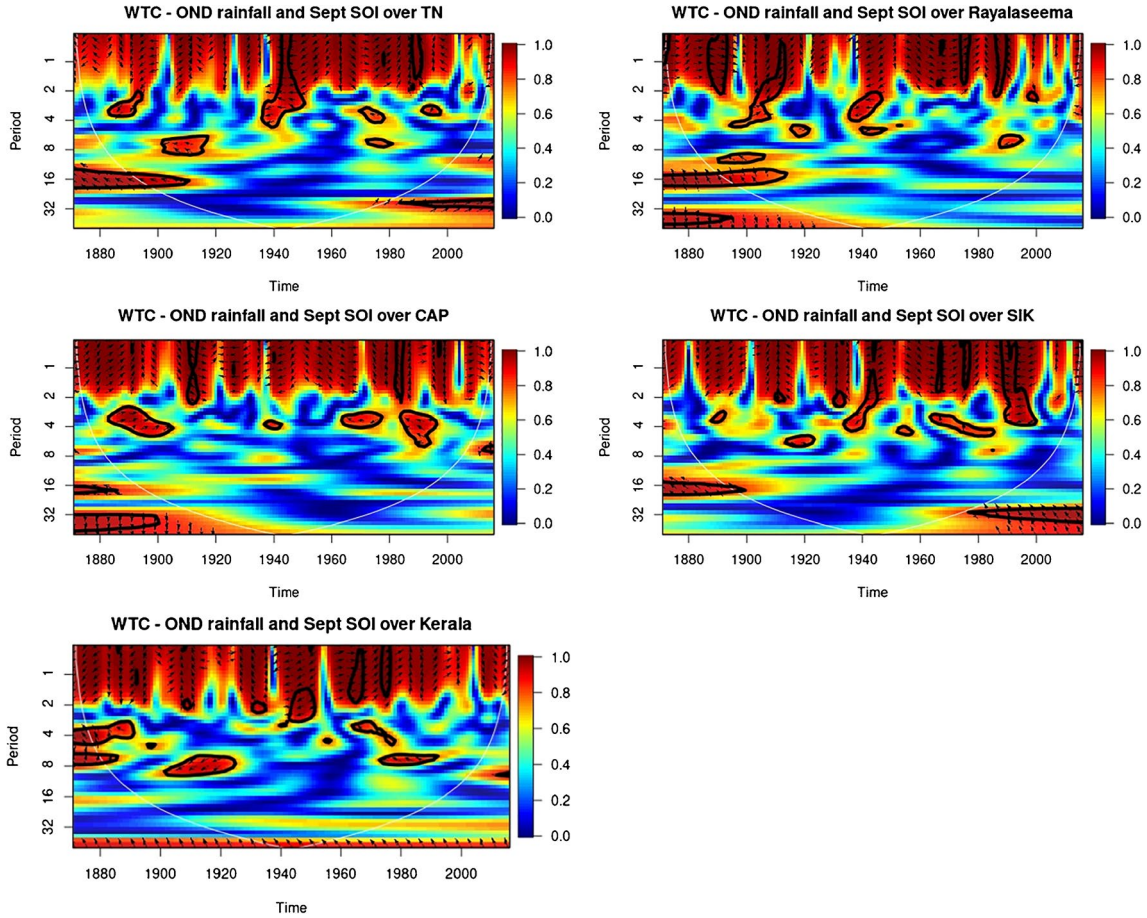

Fig. 5 Wavelet coherence between OND rainfall and September SOI over each of the five meteorological subdivisions

the periods 1900–1920 and 1980–2000. This correlation is strong at time scales of 2–4 years and 4–8 years during the periods 1880–1920, possibly related to the ENSO cycle and the oscillation of anomalous SST over the Indian Ocean.

Similarly, Fig. 4 show a very strong positive relationship between NEMR and Nino 3.4 Index, with a strengthening of the relationship observed over time. This coincides with the conclusion that the northeast monsoon has a strong interaction with the tropical ocean and atmospheric system and their recent strengthening. Researchers have found the presence of anomalous moisture transport from Bay of Bengal and equatorial Indian Ocean during El Nino, which could be the plausible reason for excess NEMR in Southern peninsular India. Furthermore, studies have shown a statistically significant multi-decadal relationship between ENSO and NEMR. Tables 1 and 2 show the correlations between OND rainfall and ENSO indices. The values marked with asterisks show significant correlation, with values marked with *** indicating the highest level of confidence. Table 2 shows a very strong significant correlation between OND rainfall and the spring (MAM) seasonal SOI index over all the rainfall subdivisions.

Figures 6 and 7 demonstrate lag correlations between the rainfall time series and each of the ENSO indices: SOI and Nino 3.4. The lagged correlations between the NE monsoon rainfall for the five meteorological subdivisions and the Nino

Table 1 Correlation table between OND rainfall and SOI. Values in bold are significant. Values marked with *** show 99% confidence, ** show 95% confidence, and * show 90% confidence using Students' *t*-test

	Sep	Oct	Nov	Dec	JF	MAM	JJAS	OND
CAP	−0.053	−0.008	0.018	0.022	−0.036	0.086	−0.002	0.012
TN	**−0.274*****	**−0.221*****	−0.094	**−0.202****	−0.033	**−0.162***	**−0.311*****	**−0.204****
SIK	**−0.167****	−0.007	0.052	−0.055	−0.031	−0.059	−0.121	−0.006
KER	**−0.244*****	**−0.167****	−0.071	−0.101	−0.109	**−0.203****	**−0.203****	−0.133
RYS	−0.071	0.005	0.091	−0.012	−0.014	−0.022	−0.069	0.031

Table 2 Correlation table between OND rainfall and Seasonal Nino 3.4. Values in bold are significant. Values marked with *** show 99% confidence, ** show 95% confidence, and * show 90% confidence using Students' *t*-test

	Oct	Nov	Dec	JF	MAM	JJAS	OND
CAP	**0.214***	**0.207***	0.185	**0.218***	**0.292****	**0.214***	**0.203***
TN	**0.222***	**0.204***	0.177	0.131	**0.267****	**0.258****	0.202
SIK	0.064	0.035	0.042	0.190	**0.255****	0.099	0.047
KER	0.182	0.186	0.174	0.100	**0.219***	0.193	0.182
RYS	0.153	0.147	0.115	0.100	0.155	0.173	0.139

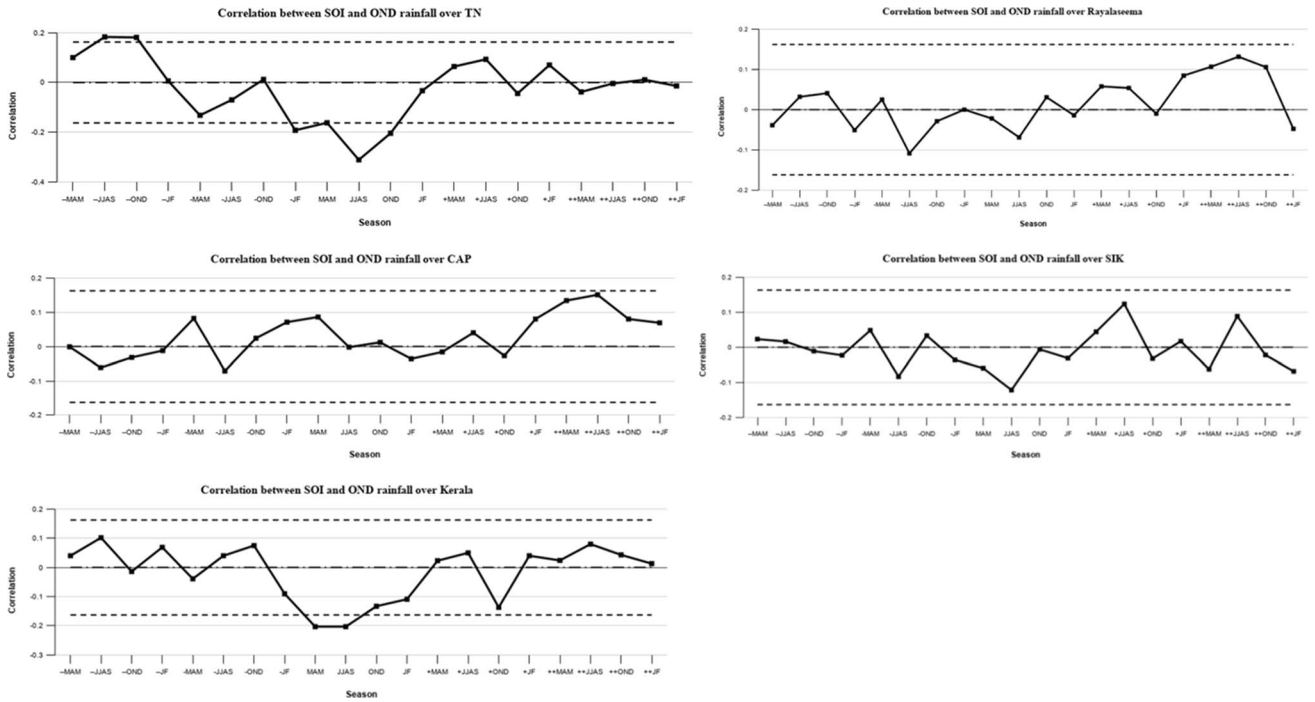

Fig. 6 Seasonal lag correlations between SOI and OND rainfall over the five rainfall subdivisions

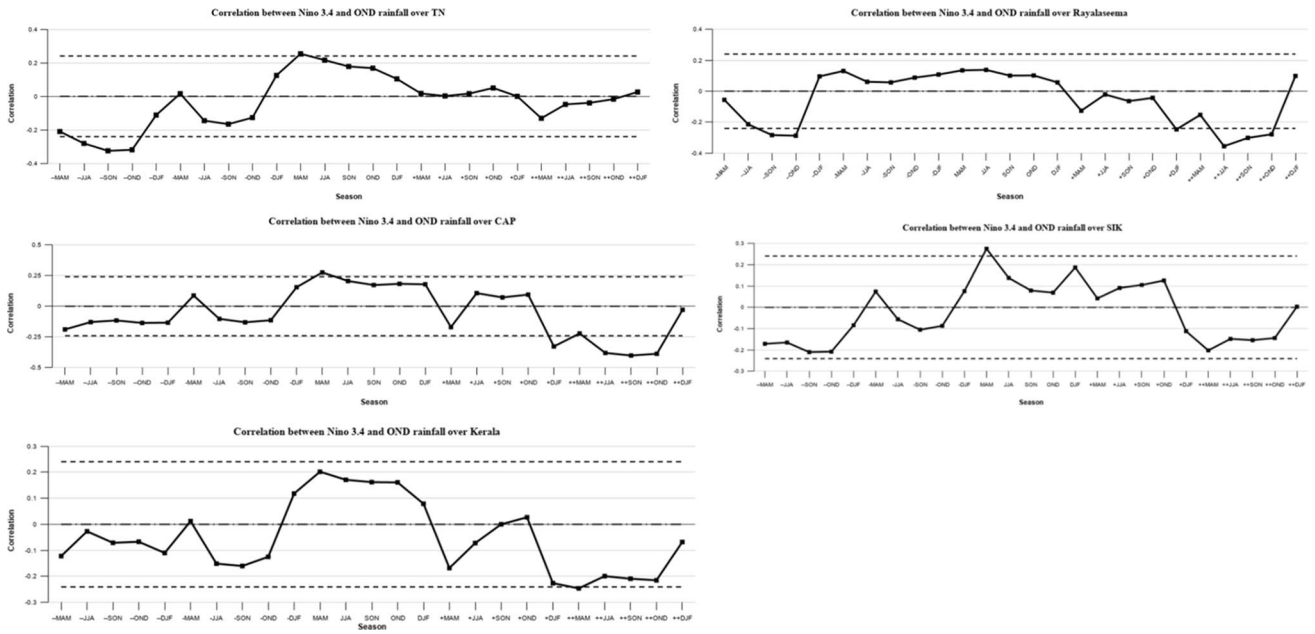

Fig. 7 Seasonal lag correlations between Nino 3.4 Index and OND rainfall over the five rainfall subdivisions

3.4 index oscillate with time. The correlations during the winter and pre-monsoon months of the previous year are negative, which changes to positive during May to October of the concurrent year and then subsequently changes to negative values. The correlation during May to October of the concurrent year is positive, whereas a strong negative relationship exists between the SOI and NEMR in antecedent and concurrent modes, which changes as the season advances and then turns positive. These changes are attributed to the modulations in the position of the subtropical ridge and the equatorial trough under the influence of the Southern Oscillation.

Teleconnection: NEMR and IOD

The Northeast Monsoon Rainfall (NEMR) in India is closely linked to the Indian Ocean Dipole (IOD), a climatic phenomenon characterized by sea surface temperature anomalies in the tropical Indian Ocean. Positive phases of IOD favor normal or above-normal NEMR, while negative phases could lead to below-normal or weak NEMR. The relationship between the two variables is particularly strong on timescales shorter than 4 years, although there are also some correlations in a 16-year timescale for specific regions such as Kerala, Rayalaseema, and Coastal Andhra Pradesh. Singh et al. (2017) further suggests that the strong gradient in sea surface temperature (SST) between the warm Western Indian Ocean and the cool Western Pacific during the Northeast monsoon season induces strong easterly wind anomalies, facilitating moisture transport towards the core Northeast monsoon region. In particular, strong positive IOD and El Niño events have been found to bring above-normal rainfall over South Peninsular India (Fig. 8).

However, caution must be exercised when interpreting the results presented in Fig. 9, which shows the seasonal lag correlation between NEMR and DMI time series. While the correlation between NEMR and DMI changes from negative to positive in the antecedent modes and remains positive in the concurrent

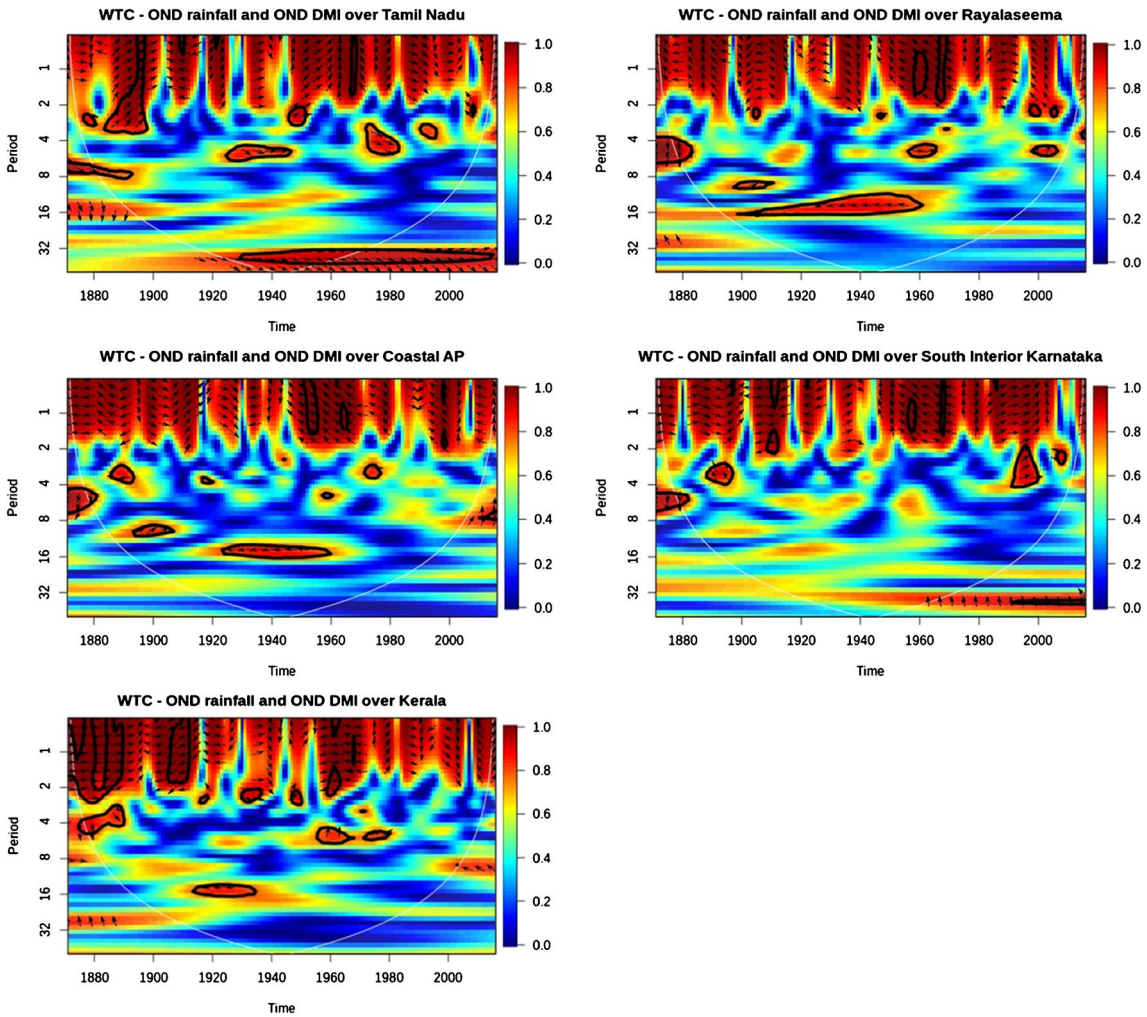

Fig. 8 Wavelet coherence between OND rainfall and DMI over each of the five meteorological subdivisions

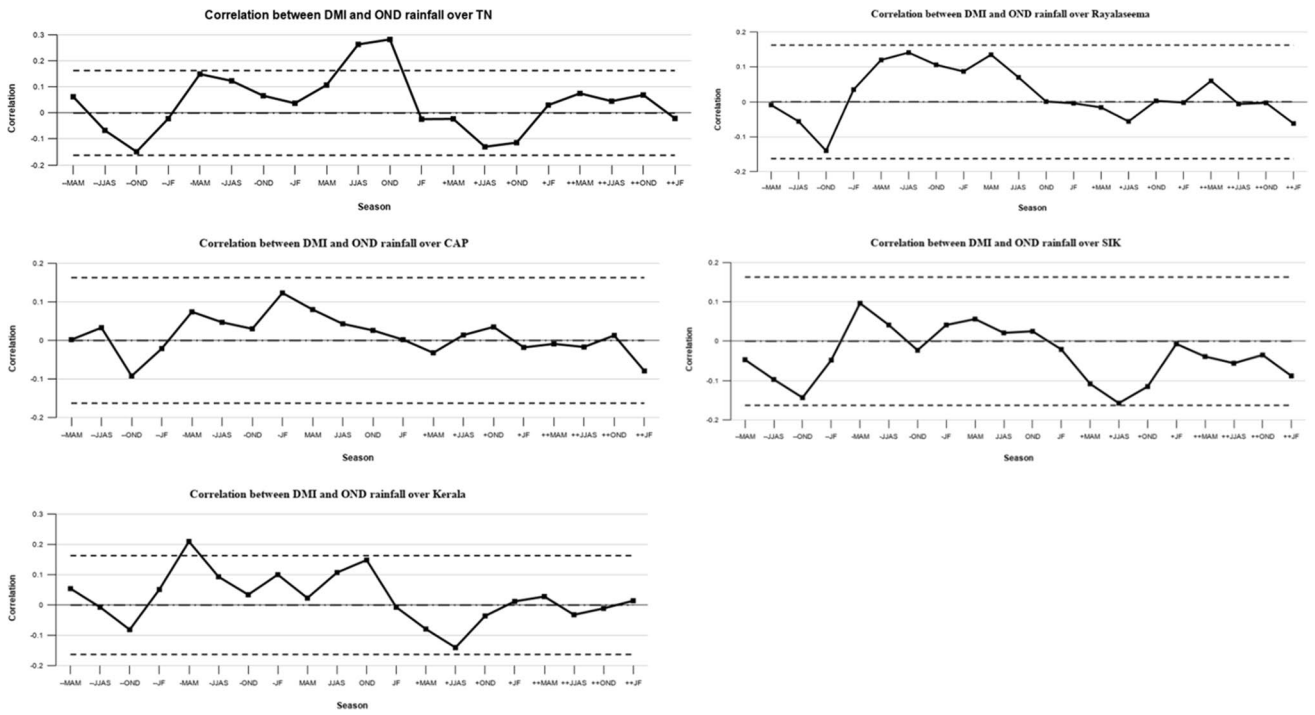

Fig. 9 Seasonal lag correlations between DMI and OND rainfall over the five rainfall subdivisions

mode, the lagged correlation between NEMR and DMI becomes negative during the subsequent monsoon. This suggests that the relationship between NEMR and DMI is not straightforward and may be influenced by other factors that are yet to be fully understood. Therefore, more research is needed to identify and assess the role of other factors in modulating the NEMR-DMI relationship, and their potential impact on the Northeast monsoon.

Overall, these findings highlight the complex interplay between oceanic and atmospheric processes that influence NEMR in India and emphasize the need for continued research to better understand and predict these phenomena for effective climate adaptation and disaster risk reduction efforts in the region.

Conclusions

This study attempts to understand the temporal characteristics of NEMR and the large-scale circulation indices and the linkage between them. To identify the dominant timescales of the variability of the northeast monsoon rainfall and the large-scale circulations, the wavelet analysis, the wavelet transform of the OND rainfall over the five rainfall subdivisions was used.

The following conclusions were obtained from the study.

a. Tamil Nadu and Kerala show strong variations at 8–16 years and 16–32 years' time scales, respectively. Strong variability at time scales of 2–4 years during the period 1871–1950 was observed. Kerala shows variations in the time scale of 16–32 years and CAP shows variability at timescales of 8–16 years during the period 1871–2000. Moreover, the variability of the ENSO cycle at time scales of 2–8 years and the variability of the DMI at time scales of 2–4 years has been observed.
b. Wavelet coherence plots show a strong negative relationship with the SOI index and a strong positive relationship with NEMR with Nino 3.4 and IOD. A strengthening of the relationship between NEMR and ENSO has been observed from the wavelet power spectrum.
c. Lagged correlations show the pattern of the correlations between the NEMR and the indices change with the season and within a lag of two years. The relationship between NEMR and SOI is negative in the precedent and antecedent modes but a reversal in the relationship is observed in the concurrent mode.

The results from the study reveal the temporal characteristics of NEMR over the five meteorological stations in the South Peninsular India and its behavior with ENSO and IOD circulation patterns. From the results, the observed time scales of variability seem to vary from interannual timescales to decadal time scales. Understanding the temporal variability of the NEMR would help in better analysis and to identify the course of the system. The associations identified between NEMR and the circulation indices are also found to be consistent with the earlier studies.

Acknowledgements The authors are thankful to the organizations from which data sets are obtained for conducting this study. The Homogeneous Indian Monthly Rainfall Data Sets (1871–2016) data have been prepared by the Indian Institute of Tropical Meteorology (IITM) from instrumental records maintained by the Meteorological Department (IMD). The data on the circulation indices are obtained from the NOAA ESRL Physical Sciences Laboratory and Climatic Research Unit under University of East Anglia. The authors would like to express their sincere thanks to Mr. Unashish Mondal for his invaluable assistance in correcting the typography and grammar errors in this manuscript.

Author contribution Harithasree S: conceptualization, methodology, investigation, writing—original draft. S. K. Panda: supervision, funding acquisition, conceptualization, writing—review and editing. K. C. Pattnayak: investigation, writing—review and editing.

Funding SKP is supported by the University Grant Commission (UGC) through the UGC-BSR Research Start Up Grant (No. F.30 – 414/2018(BSR)) under which this research has been conducted.

Data availability All data used in this study are freely available obtained directly from the source: Homogeneous Indian Monthly Rainfall dataset https://www.tropmet.res.in/data/data-archival/rain/iitm-subdivrf.txt for precipitation data. The circulation indices (i) SOI was taken from https://crudata.uea.ac.uk/cru/data/soi/ maintained by Climate Research Unit under University of East Anglia, (ii) Nino 3.4 Index was taken from https://psl.noaa.gov/data/correlation/nina34.anom.data and (iii) DMI was taken from https://psl.noaa.gov/gcos_wgsp/Timeseries/DMI/ both maintained by NOAA Physical Research Laboratory.

Declarations

Competing interest The authors declare no competing interests.

References

Aguiar-Conraria L, Soares MJ (2011) The continuous wavelet transform: a primer, No 16/2011, NIPE Working Papers, NIPE - Universidade do Minho. https://EconPapers.repec.org/RePEc:nip:nipewp:16/2011

Ashok K, Guan Z, Yamagata T (2001) Impact of Indian Ocean dipole on the relationship between the Indian Monsoon Rainfall and ENSO. Geophys Res Lett - Geophys Res Lett 28(23):4499–502. https://doi.org/10.1029/2001GL013294

Balachandran S, Geetha B, Ramesh K, Deepa RV, Mourya YP, Rakhil KS (2020) Regional Meteorological Centre, Chennai, IMD Chennai Scientific Report No. IMDC-SR/08, Report on Northeast Monsoon – 2019. https://mausam.imd.gov.in/chennai/mcdata/ne_monsoon_2019.pdf

Bjerknes J (1966) A possible response of the atmospheric Hadley circulation to equatorial anomalies of ocean temperature. Tellus 18:820–829. https://doi.org/10.1111/j.2153-3490.1966.tb00303.x

Bjerknes J (1969) Atmospheric teleconnections from the equatorial pacific. Mon Weather Rev 97(3):163–172. https://doi.org/10.1175/1520-0493(1969)097%3c0163:ATFTEP%3e2.3.CO;2

Chang C, Glover GH (2010) Time-frequency dynamics of resting-state brain connectivity measured with fMRI. Neuroimage 50(1):81–98. https://doi.org/10.1016/j.neuroimage.2009.12.011

Das S, Tomar CS, Saha D, Shaw SO, Singh C (2015) Trends in rainfall patterns over north-East India during 1961–2010. Int J Earth Atmos Sci 2:37–48

Das S, Bhattacharjee K, Shaw SO, Pathak HG, Patowary B (2011) Characteristic pattern and recent trend in rainfall over Guwahati. Proceedings of "Water for Cities: responding to the Urban Challenges". Guwahati

Deka RL, Mahanta C, Pathak H, Nath KK, Das S (2013) Trends and fluctuations of rainfall regime in the Brahmaputra and Barak basins of Assam. India Theor Appl Climatol 114:61–71

Dhar ON, Rakhecha PR (1983) Forecasting northeast monsoon rainfall over Tamil Nadu. India Mon Weather Rev 111:109–112

Geetha B, Raj YEA (2015) A 140 years data archive of dates of onset and withdrawal of northeast monsoon over coastal Tamil Nadu: 1871–2010 (Re-determination for 1901–2000). Mausam 66(1):7–18

George G, Charlotte BV, Ruchith RD (2011) Interannual variation of northeast monsoon rainfall over southern peninsular India. Indian J Geo-Marine Sci 40:98–104. https://doi.org/10.1002/met.1322

Goswami BN, Ajayamohan RS, Xavier PK, Sengupta D (2003) Clustering of synoptic activity by Indian summer monsoon intraseasonal oscillations. Geophys Res Lett 30(8):1431. https://doi.org/10.1029/2002GL016734

Goswami BN, Venugopal N, Sengupta D, Madhusoodanan MS, Xavier PK (2006) Increasing trend of extreme rain events over India in a warming environment. Science 314:1442–1445. https://doi.org/10.1126/sci-ence.1132027

Hansen J, Sato M, Glascoe J, Ruedy R (1998) A common-sense climate index: is climate changing noticeably? Proc Natl Acad Sci 95:4113–4120

Harris I, Jones PD, Osborn TJ, Lister DH (2014) Updated high-resolution grids of monthly climatic observations. Int J Climatol 34:623–642. https://doi.org/10.1002/joc.3711

Hu ZZ, Nitta T (1996) Wavelet analysis of summer rainfall over North China and India and SOI using 1891–1992 data. J Meteorol Soc Jpn 74:833–844. https://doi.org/10.2151/jmsj1965.74.6_833

Jain SK, Kumar V, Saharia M (2013) Analysis of rainfall and temperature trends in Northeast India. Int J Climatol 33:968–978

Kripalani RH, Kumar P (2004) Northeast monsoon rainfall variability over south peninsular India vis-à-vis the Indian Ocean dipole mode. Int J Climatol 24:1267–1282. https://doi.org/10.1002/joc.1071

Kumar A, Hoerling MP (2003) The nature and causes for the delayed atmospheric response to El Niño. J Clim 16(9):1391–1403

Kumar P, Kumar K, Rajeevan M, Sahai A (2007) On the recent strengthening of the relationship between ENSO and northeast monsoon rainfall over South Asia. Clim Dyn 28:649–660. https://doi.org/10.1007/s00382-006-0210-0

Madden RA, Julian PR (1971) Detection of a 40–50 day oscillation in the zonal wind in the tropical Pacific. J Atmos Sci 28:702–708

Madden RA, Julian PR (1972) Description of global-scale circulation cells in the tropics with a 40–50 day period. J Atmos Sci 29:1109–1123

Parthasarathy B, Rupa Kumar K, Munot AA (1993) Homogeneous Indian Monsoon Rainfall: variability and prediction. Proc Indian Acad Sci 102(1):121–155

Raj YEA, Geetha B (2008) Relation between southern oscillation index and Indian northeast monsoon as revealed in antecedent and concurrent modes. Mausam 59(1):15–34. https://doi.org/10.54302/mausam.v59i1.1129

Rajeevan M, Unnikrishnan CK, Bhate J, Niranjan Kumar K, Sreekala PP (2012) Northeast monsoon over India: variability and prediction. Met Apps 19:226–236

Rao YP (1976) Southwest Monsoon, vol 1. India Meteorological Department, New Delhi, India

Rathinasamy M, Agarwal A, Sivakumar B et al (2019) Wavelet analysis of precipitation extremes over India and teleconnections to climate indices. Stoch Environ Res Risk Assess 33:2053–2069. https://doi.org/10.1007/s00477-019-01738-3

Saji NH, Goswami BN, Viayachandran PN, Yamagata T (1999) A dipole mode in the tropical Indian ocean. Nature 401:360–363

Schmidbauer H, Roesch A (2018) WaveletComp 1.1: A guided tour through the R package

Schneider DP, Deser C, Fasullo J, Trenberth KE (2013) Climate data guide spurs discovery and understanding. Eos Trans AGU 94(13):121

Singh P, Gnanaseelan C, Chowdary JS (2017) North-East monsoon rainfall extremes over the southern peninsular India and their association with El Nino. Dynamics of Atmospheres and Oceans. 1–11.https://doi.org/10.1016/j.dynatmoce.2017.08.002

Tomita T, Yasunari T (1996) Role of the northeast winter monsoon on the biennial oscillation of the ENSO/monsoon system. J Meteor Soc Japan 74(4):399–413

Torrence C, Compo GP (1998) A practical guide to wavelet analysis. Bull Am Meteor Soc 79(1):61–78

Walker GT (1924) Correlation in Seasonal Variations of Weather, IX. A Further Study of World Weather". Miami India Meteorol Depart 24(9):275–333

Yasunari T, Seki Y (1992) Role of the Asian monsoon on the interannual variability of the global climate system. J Meteorol Soc Jpn 70:177–189. https://doi.org/10.2151/jmsj1965.70.1B_177

Zubair L, Ropelewski CF (2006) The strengthening relationship between ENSO and northeast monsoon rainfall over Sri Lanka and southern India. J Clim 19(8):1567–1575